Heat release in glasses at low temperatures

D. A. Parshin*
Institut für Angewandte Physik der Universität Heidelberg, Albert-Überle-Strasse 3-5, 6900 Heidelberg, Germany

S. Sahling
Institut für Tieftemperaturphysik, Technische Universität Dresden, Mommsenstrasse 13, O-8027 Dresden, Germany
(Received 27 July 1992)

The long-time heat release in glasses after cooling a sample from some initial temperature T_1 to T_0 has been calculated in the framework of the soft-potential model. It is shown that there are three temperature regions where time and temperature dependences of the heat release are different. In the thermal activation region $T_0 > T_c$ (where T_c is a characteristic crossover temperature from tunneling to activation of the order of a few kelvin) the heat release appears to be independent of T_1 and proportional to $T_0^{9/4}\ln(t/t_0)/t \approx T_0^{9/4}/t^{0.76}$ for $t > t_0$, where t_0 is of the order of 100 s. In the tunneling region $T_1 < T_c$ the heat release is proportional to $(T_1^2 - T_0^2)/t$ in accordance with a prediction of the standard tunneling model. And in the intermediate region $T_0 < T_c < T_1$ the heat release is proportional to $(T_c^2 - T_0^2)/t$ and does not depend on T_1. It is shown that there is a distribution of the characteristic crossover temperature in the glass. This distribution can be calculated from the heat-release data in the intermediate temperature region. The distribution function has several peaks corresponding to several types of two-level systems in the glass. Choosing these distributions it is possible to explain the numerous heat-release experiments in different materials.

I. INTRODUCTION

It is well known now that two-level systems (TLS's) are responsible for the universal low-temperature properties of glasses,[1] and the model of Anderson, Halperin, Varma, and Phillips[2,3] (AHVP model) explains these properties quite well. However, the region of applicability of this model is limited to low temperatures only (below a few kelvin). At higher temperatures predictions of the AHVP model contradict with experimental data. This also takes place in those cases when it is clear that the TLS's are responsible for the observable phenomena. One of them is the long-time heat release. The TLS's with high barriers V (and large relaxation times) are responsible for the long-time dependence of the heat release in glasses.[4,5]

The heat release $\dot{Q}$ is usually measured after cooling a sample from some initial equilibrium temperature T_1 (charging temperature) to a final temperature T_0. According to the AHVP model, the temperature and time dependences of the heat release are[4]

$$\dot{Q} \propto \frac{T_1^2 - T_0^2}{t} ; \tag{1.1}$$

i.e., it increases with T_1 proportional to $T_1^2 - T_0^2$. However, such temperature dependence is usually observed if T_1 is smaller than a few kelvin only. For higher charging temperatures, the heat release saturates and does not depend on T_1.[6-18]

There are at least two possibilities to explain this behavior. First, the distribution function of the TLS's energies E has a cutoff at some energy E_f of the order of a few kelvin[7] and the TLS's density of states, $\bar{P}=0$, for $E > E_f$. Second, for temperatures T_1 higher than some characteristic temperature T_c (also of the order of a few kelvin), it is impossible to create a nonequilibrium distribution of the TLS's during the cooling of the sample from T_1 to T_c. The reason is that there are fast-relaxation processes in this temperature region in the TLS's responsible for the heat release at $T = T_0$ on the experimental time scale.[6,19] The mechanism of the fast relaxation can be thermal activation processes over the barrier. It is known that these processes are responsible for the relaxation ultrasound absorption in glasses at temperatures above a few kelvin.[20] But the AHVP model gives no answer about the value of the crossover temperature T_c from tunneling to activation, and in the framework of this model it is not clear why the crossover temperature T_c is so small (of the order of a few kelvin).

But it is possible to answer this question in the framework of the soft-potential model (SPM), which has been proposed in Ref. 21 and developed further in Refs. 22–28. The SPM contains the AHVP model as a particular case and reproduces at low temperatures all the results of the AHVP model concerning the universal low-temperature properties of glasses.[25] The advantage of this model is that without additional hypotheses it describes the higher-temperature universal properties of glasses too.[23,24,26-28]

II. SOFT-POTENTIAL MODEL

According to the soft-potential model,[21] the TLS's are described by the soft anharmonic-oscillator potentials

$$V(x) = \mathcal{E}_0 \left[\eta \left[\frac{x}{a} \right]^2 + \xi \left[\frac{x}{a} \right]^3 + \left[\frac{x}{a} \right]^4 \right] . \tag{2.1}$$

Here x is the generalized coordinate having the units of length and describing the motion of the tunneling entity, a is the characteristic length of the order of the interatomic spacing ($a \simeq 1$ Å), and $\mathcal{E}_0$ is the binding energy of the order of $\bar{M}v^2 \simeq 10$ eV, $\bar{M}$ being the average mass of atoms constituting the glass. The values of the dimensionless parameters η and ξ are distributed due to fluctuations of the structural parameters of a glass. The soft potentials correspond to $|\eta|, |\xi| \ll 1$. In this region the distribution function of these parameters is given by[23]

$$P(\eta,\xi)=\frac{|\eta|}{2}\mathcal{P}_0 , \tag{2.2}$$

where $\mathcal{P}_0$ is a constant.

For $\xi^2/\eta_L < \eta_L/|\eta|$, negative η, and $|\eta| > 3\eta_L$,[25] the two lowest levels in the potential (2.1) form a TLS with the energy splitting E,

$$E=(\Delta_0^2+\Delta^2)^{1/2} . \tag{2.3}$$

The tunneling splitting Δ_0 and the asymmetry Δ are determined by

$$\Delta_0 \approx W \exp\left[-\frac{\sqrt{2}}{3}\left[\frac{|\eta|}{\eta_L}\right]^{3/2}\right] , \tag{2.4}$$

$$\Delta=\frac{W}{\sqrt{2}}\frac{|\xi|}{\sqrt{\eta_L}}\left[\frac{|\eta|}{\eta_L}\right]^{3/2} , \tag{2.5}$$

where η_L is the important small parameter of the model,

$$\eta_L=(\hbar^2/2Ma^2\mathcal{E}_0)^{1/3} \approx 10^{-2} , \tag{2.6}$$

M being an effective mass of the tunneling entity. The energy W is determined by

$$W=\mathcal{E}_0\eta_L^2 \approx k(10\ \mathrm{K}) , \tag{2.7}$$

where k is the Boltzmann constant. This is the scale of characteristic energies in the potential (2.1) for $\eta=\xi=0$. The barrier height V between two minima in the double-well potential (2.1) for $\Delta \ll V$ depends on the value of $|\eta|$ only:

$$V=\frac{W}{4}\left[\frac{\eta}{\eta_L}\right]^2 . \tag{2.8}$$

The interaction of the soft atomic potential (2.1) with a deformation ε is described by the bilinear term[25,26,28]

$$V_{\mathrm{int}}=\mathcal{E}_0 H\left[\frac{x}{a}\right]\varepsilon , \tag{2.9}$$

where the dimensionless coefficient $H \simeq 1$. The deformation potential of the TLS γ is given by[25,26]

$$|\gamma|=\frac{1}{\sqrt{2}}\frac{HW}{\eta_L^{3/2}}\left[\left|\frac{\eta}{\eta_L}\right|\right]^{1/2} . \tag{2.10}$$

It appears to be of the order of 1 eV.

In the tunneling region the TLS relaxation time is given by the usual expression

$$\left[\frac{1}{\tau}\right]_{\mathrm{tun}}=\frac{\Delta_0^2 E\gamma^2}{2\pi\rho\hbar^4 v^5}\coth\frac{E}{2kT} \equiv \frac{1}{\tau(E)}\exp\left[-\frac{8}{3}\left[\frac{V}{W}\right]^{3/4}\right] , \tag{2.11}$$

where

$$\tau(E)=\frac{2\pi\rho\hbar^4 v^5}{W^2\gamma^2 E}\tanh\frac{E}{2kT} , \tag{2.12}$$

and we take into account (2.4) and (2.8). In the thermal activation region, the relaxation time

$$\left[\frac{1}{\tau}\right]_{\mathrm{act}}=\frac{1}{\tau_0}e^{-V/kT} , \tag{2.13}$$

where $\tau_0 \simeq 10^{-12}-10^{-13}$ s.

The crossover temperature T_c from tunneling to activation can be found from the equations

$$\left[\frac{1}{\tau}\right]_{\mathrm{tun}}=\left[\frac{1}{\tau}\right]_{\mathrm{act}}=\frac{1}{t} , \tag{2.14}$$

where t is a time of experiment. As a result,[29]

$$kT_c=\left[\frac{3}{8}\right]^{4/3} W\frac{\ln^{4/3}[t/\tau(E)]}{\ln(t/\tau_0)} . \tag{2.15}$$

For $t=100$ s, $\tau(E)=10^{-11}$ s, and $\tau_0 \simeq 10^{-13}$ s, $kT_c=0.73W$.

Just the smallness of the energy W explains the smallness of the crossover temperature T_c from tunneling to activation. The value W for a particular glass can be obtained from the position of the minimum T_{min} in the temperature dependence of $C(T)/T^3$, where $C(T)$ is the specific heat.[23,24] From numerical calculations[23] (see also Ref. 24), it has been found that $kT_{\mathrm{min}}/W \approx 0.4-0.5$ (depending on the details of the distribution function of η if $\mathcal{P}_0$ is not a constant), i.e.,

$$W \approx (2-2.5)kT_{\mathrm{min}} . \tag{2.16}$$

For SiO_2, $T_{\mathrm{min}} \approx 2$ K, i.e., $W/k \approx 4-5$ K and $T_c \approx 2.9-3.7$ K.

III. GENERAL THEORY OF THE HEAT RELEASE IN GLASSES

The general formula for the heat release in glasses due to TLS's reads

$$\dot{Q}=-\sum_{\mathrm{TLS}}\dot{n}E=\sum_{\mathrm{TLS}}\frac{n-n_0}{\tau}E , \tag{3.1}$$

where n is the TLS upper-level occupation number, n_0 is the equilibrium upper-level occupation number, and τ is the TLS relaxation time.

The heat release at the temperature T_0 as a function of time t ($t=0$ corresponds to the final temperature T_0) is then given by

$$\dot{Q}=\sum_{\mathrm{TLS}}\frac{E}{\tau}[n(0)-n_0]e^{-t/\tau} , \tag{3.2}$$

where $n(0)$ is the nonequilibrium occupation number at the moment $t=0$, n_0 is the equilibrium occupation number at the temperature T_0,

$$n_0=\frac{1}{e^{E/kT_0}+1} , \tag{3.3}$$

and τ is the TLS relaxation time at $T=T_0$.

Let us calculate the heat release and discuss the results for three different cases: (1) $T_0,T_1<T_c$ (the thermal activation processes can be neglected), (2) $T_c<T_0,T_1$ (the thermal activation processes dominate), and (3) $T_0<T_c<T_1$ (the intermediate case).

A. Tunneling range ($T_0,T_1<T_c$)

In the tunneling range, we can take the nonequilibrium occupation number $n(0)$ in the equilibrium form at the initial temperature T_1,

$$n(0)=\frac{1}{e^{E/kT_1}+1} . \tag{3.4}$$

To calculate the heat release in this case, we will use instead of the variables η and ξ those of the AHVP model,

$$E \text{ and } p=\left[\frac{\Delta_0}{E}\right]^2 . \tag{3.5}$$

Now, taking into account that $P(\eta,\xi)$ is an even function of ξ, we obtain from (2.2)–(2.5) the distribution function $F(E,p)$ of variables E and p:[25]

$$F(E,p)=\left[\frac{2}{9}\right]^{1/3}\frac{\mathcal{P}_0\eta_L^{5/2}}{W}\frac{1}{p\sqrt{1-p}}\frac{1}{L^{2/3}} , \tag{3.6}$$

where

$$L=\ln\frac{W}{E\sqrt{p}} . \tag{3.7}$$

The distribution function practically does not depend on the TLS energy E.

The relaxation time (2.11) can be expressed through the same variables too,

$$\left[\frac{1}{\tau}\right]_{\text{tun}}=p\frac{\gamma^2E^3}{2\pi\rho\hbar^4v^5}\coth\frac{E}{2kT}\equiv\frac{p}{\tau_{\min}(E)} , \tag{3.8}$$

where we will neglect in the following the logarithmical dependence of the minimal relaxation time $\tau_{\min}(E)$ on parameter p [through the deformation potential γ; see (2.10)].

Replacing the summation in (3.2) by the integration with the distribution function $F(E,p)$,

$$\sum_{\text{TLS}}\cdots=\mathcal{V}\int_0^\infty dE\int_0^1 dp\,F(E,p) , \tag{3.9}$$

where $\mathcal{V}$ is the volume of the glass, and integrating over p and then over E,

$$\int_0^\infty dE\frac{E}{e^{E/kT}+1}=\frac{\pi^2k^2}{12}T^2 , \tag{3.10}$$

we obtain, for $t\gg\tau_{\min}(kT_0)$,

$$\dot{Q}=\frac{\pi^2k^2}{12}\left[\frac{2}{9}\right]^{1/3}\times\frac{\mathcal{P}_0\eta_L^{5/2}}{W}\mathcal{V}[T_1^2f(T_1,t)-T_0^2f(T_0,t)]t^{-1} , \tag{3.11}$$

where

$$f(T,t)=\ln^{-2/3}\left[\frac{W}{kT}\left[\frac{t}{\tau_{\min}(kT)}\right]^{1/2}\right] . \tag{3.12}$$

So the heat release in the tunneling region is roughly proportional to $(T_1^2-T_0^2)/t$. Such dependence is equivalent to the AHVP model (1.1).

B. Thermal activation range ($T_c<T_0,T_1$)

For the thermal activation processes, the relaxation time $\tau=\tau_0e^{V/kT_0}$ [see (2.13)]. Because of its strong temperature dependence, the relaxation time may change by many orders of magnitude for temperature changes of a few kelvin. Because of this, any realistic cooling schedule will inevitably lead to a nonequilibrium situation. It has been shown that there is a characteristic freezing temperature T^*; above this temperature the TLS occupation number coincides with its equilibrium value n_0, and below it is given by its frozen-in value at $T=T^*$.[30–33] In accordance with Ref. 33, the width of the transition region, where freezing takes place, is much smaller than the freezing temperature and the occupation number n (for TLS's with $E\ll V$) as a function of time during cooling of the sample from T_1 to T_0 (for arbitrary cooling schedule) is given by

$$n(t)=\begin{cases}n_0(t) & \text{for } t<t^* ,\\ n_0(t^*) & \text{for } t>t^* ,\end{cases} \tag{3.13}$$

where t^* is defined by $T(t^*)=T^*$ and T^* is the freezing temperature,[33]

$$kT^*=V\Big/\ln\left[\frac{kT^{*2}}{\tau_0V|R^*|}\frac{1+e^{-E/kT^*}}{\ln2}\right] , \tag{3.14}$$

where $|R^*|$ is the cooling rate at the freezing temperature T^*.

So the occupation of the upper level of the TLS is given by the equilibrium value for $T>T^*$ and by the frozen-in value $n_0(T^*)$ for $T<T^*$. Therefore TLS's with $T^*<T_0$ do not contribute to the heat release at all because their occupation number $n(0)$ coincides with the equilibrium value n_0. Hence

$$\dot{Q}=\sum_{\text{TLS}}\frac{E}{\tau}\left[\frac{1}{e^{E/kT^*}+1}-\frac{1}{e^{E/kT_0}+1}\right]e^{-t/\tau}\Theta(T^*-T_0) , \tag{3.15}$$

where $\Theta(x)$ is the Heaviside step function [$\Theta(x)=1$ for $x>0$ and $\Theta(x)=0$ for $x<0$].

In the thermal activation region, we will use for calculations the variables E and V instead of variables η and ξ. The corresponding distribution function $\Phi(E,V)$ can be

calculated from (2.2), (2.5), and (2.8) if we neglect the tunneling splitting Δ_0. As a result,

$$\Phi(E,V)=\frac{\mathcal{P}_0\eta_L^{5/2}}{W^{5/4}V^{3/4}} . \tag{3.16}$$

Replacing the summation in (3.15) by the integration with the distribution function $\Phi(E,V)$,

$$\sum_{\text{TLS}} \cdots = \mathcal{V}\int_0^\infty dV \int_0^\infty dE\, \Phi(E,V) , \tag{3.17}$$

and integrating over the energy using (3.10) (one may neglect the weak energy dependence of the freezing temperature), we obtain

$$\dot{Q}=\frac{\pi^2 k^2}{12}\frac{\mathcal{P}_0\eta_L^{5/2}}{W^{5/4}}\mathcal{V}\int_0^\infty \frac{dV}{V^{3/4}}\frac{1}{\tau}e^{-t/\tau}(T^{*2}-T_0^2) \times\Theta(T^*-T_0) . \tag{3.18}$$

To carry out the integration in (3.18), let us change the integration variable V for τ,

$$V=kT_0\ln\frac{\tau}{\tau_0} \quad \text{and} \quad dV=kT_0\frac{d\tau}{\tau} . \tag{3.19}$$

It follows from (3.14) and (3.19) that

$$kT^*\approx V\Big/\ln\left[\frac{kT^{*2}}{\tau_0|R^*|V}\right] =kT_0\ln(\tau/\tau_0)\Big/\ln\left[\frac{T^{*2}}{\tau_0|R^*|T_0\ln(\tau/\tau_0)}\right] . \tag{3.20}$$

The lower limit t_0 of integration over τ is determined by the condition $T^*=T_0$. We obtain, from (3.20),

$$t_0=\frac{T_0}{|R^*|\ln(t_0/\tau_0)}\approx\frac{T_0}{|R^*|\ln(T_0/|R^*|\tau_0)} \tag{3.21}$$

($t_0\simeq 30$ s for the heat-release experiments in the thermal activation range $T_0=10$ K, $|R^*|=10^{-2}$ K/s, and $\tau_0=10^{-13}$ s). And, for $T^*(\tau>t_0)$, we will use the expression [see (3.20)]

$$T^*\approx T_0\frac{\ln(\tau/\tau_0)}{\ln(t_0/\tau_0)} . \tag{3.22}$$

Because, as follows from (3.20) for realistic relaxation time $\tau<10^6$ s, $T_0<T^*<1.3T_0$, instead of T^*, we can set T_0 in the denominator of (3.20). As a result

$$\dot{Q}=\frac{\pi^2}{12}\frac{\mathcal{P}_0\eta_L^{5/2}}{W}\frac{W^2}{\ln^2(t_0/\tau_0)}\left[\frac{kT_0}{W}\right]^{9/4}\mathcal{V} \times\int_{t_0}^\infty\frac{d\tau}{\tau^2}e^{-t/\tau}\frac{\ln^2(\tau/\tau_0)-\ln^2(t_0/\tau_0)}{\ln^{3/4}(\tau/\tau_0)} . \tag{3.23}$$

Replacing the integration variable once again,

$$\frac{t}{\tau}=y \quad \text{and} \quad d\tau=-t\frac{dy}{y^2} , \tag{3.24}$$

we derive

$$\dot{Q}=\frac{\pi^2}{12}\frac{\mathcal{P}_0\eta_L^{5/2}}{W}\frac{W^2}{\ln^2(t_0/\tau_0)}\left[\frac{kT_0}{W}\right]^{9/4}\frac{\mathcal{V}}{t} \times\int_0^{t/t_0}dy\, e^{-y}\frac{\ln^2(t/\tau_0 y)-\ln^2(t_0/\tau_0)}{\ln^{3/4}(t/\tau_0 y)} . \tag{3.25}$$

For $t\gg t_0$ we can replace the upper limit in the integral (3.25) by infinity. Performing the integration, we obtain

$$\dot{Q}=\frac{\pi^2}{6}\frac{\mathcal{P}_0\eta_L^{5/2}}{W}\frac{W^2}{\ln^2(t_0/\tau_0)}\left[\frac{kT_0}{W}\right]^{9/4}\mathcal{V} \times\frac{\ln(tt_0/\tau_0^2)^{1/2}}{\ln^{3/4}(t/\tau_0)}\frac{\ln(t/t_0)}{t} . \tag{3.26}$$

Since $1\ll t/t_0\ll t/\tau_0$, we have

$$\ln\frac{t}{\tau_0}\approx\ln\frac{t_0}{\tau_0} \tag{3.27}$$

and we come to the final result

$$\dot{Q}=\frac{\pi^2}{6}\frac{\mathcal{P}_0\eta_L^{5/2}}{W}\frac{W^2}{\ln^{7/4}(t_0/\tau_0)}\left[\frac{kT_0}{W}\right]^{9/4}\mathcal{V}\frac{\ln(t/t_0)}{t} \propto T_0^{9/4}\frac{\ln(t/t_0)}{t} . \tag{3.28}$$

On the time scale $20<t/t_0<200$, the time dependence of the heat release (3.28) can be approximated by the power law $\dot{Q}\propto t^{-0.76}$ with the accuracy about of 5%. Another important thing is that the heat release in the thermal activation region does not depend on the initial temperature T_1. The physical reason is the following.

From (3.23) [see also (3.25)], it is clear that TLS's with relaxation times $\tau\approx t$ are responsible for the heat release at the moment t. The freezing temperature for these TLS's is determined by (3.22) with $\tau\approx t$. A ratio

$$\frac{\Delta T}{T_0}\equiv\frac{T^*-T_0}{T_0}\approx\frac{\ln(t/t_0)}{\ln(t_0/\tau_0)}\ll 1 \tag{3.29}$$

is much smaller than unity. For example, for $t=10^6$ s, $t_0=100$ s, and $\tau_0=10^{-13}$ s, the ratio $\Delta T/T_0\approx 0.3$. Therefore the contribution to the heat release on the realistic time scale comes from the TLS's with freezing temperatures nearly coinciding with T_0 ($T_0<T^*<1.3T_0$). The TLS's with $T^*\approx T_1>1.3T_0$ give contribution to the heat release for astronomical values of the time $t\simeq t_0(t_0/\tau_0)^{T_1/T_0-1}$ only.

We see that in comparison to the tunneling range all dependences of the heat release on the experimental parameters T_1, T_0, and t change, if the thermal activation dominates. The time dependence changes from $\dot{Q}\propto t^{-1}$ to $\dot{Q}\propto t^{-a}$ with $a<1$. In the tunneling range, the heat release is independent of T_0 (for $T_0\ll T_1$) and proportional to T_1^2 [see (3.11)]. The thermal activation converts these dependences: The heat release is independent of T_1 (at least for $T_1>1.3T_0$) and proportional to $T_0^{9/4}$ (i.e., roughly proportional to T_0^2).

C. Intermediate case ($T_0 < T_c < T_1$)

Usually from experiment, we have an intermediate case

$$T_0 < T_c < T_1 , \tag{3.30}$$

where the thermal activation processes at temperature T_0 are frozen in and the tunneling processes are responsible for the heat release. Since at $T_1 > T_c$, the thermal activation processes dominate and the nonequilibrium occupation number $n(0)$ is given by its frozen-in value $n_0(T^*)$. The formula for the heat release in this case coincides with (3.11), where instead of T_1 we should set T^*.

However, for such a conclusion one needs the condition $T^* \geq T_c$ for all the relevant TLS's. We will show now that the freezing temperature T^* depends only weakly on the relaxation (or measuring) time and TLS energy, and nearly coincides with the crossover temperature T_c (being bigger than T_c). Using (2.11), we obtain the relation between the tunneling time τ and the barrier height V:

$$V(\tau) = \left[\frac{3}{8}\right]^{4/3} W \ln^{4/3}\frac{\tau}{\tau(E)} . \tag{3.31}$$

For the freezing temperature, we will use the expression (3.14),

$$kT^* \approx \frac{V}{\ln(kT^{*2}/\tau_0|R^*|V)} = \frac{V}{L(V/\tau_0|R^*|k)} , \tag{3.32}$$

where the function $L(x)$ is determined by

$$L(x) = \ln\frac{x}{\ln^2\frac{x}{\ln^2\frac{x}{\ddots}}} . \tag{3.33}$$

Using now (2.15), (3.32), and (3.31), we obtain for the ratio T^*/T_c as a function of time ($\tau = t$),

$$\frac{T^*}{T_c} = \frac{\ln(t/\tau_0)}{L(V(t)/\tau_0|R^*|k)} . \tag{3.34}$$

For $\tau_0 = 10^{-13}$ s, $\tau(E) = 10^{-11}$ s, $|R^*| = 10^{-2}$ K/s, and $W/k = 4$ K, we obtain that this ratio changes from 1.1 to 1.4, when t changes from 10^2 to 10^6 s and it is nearly independent of W and E.

Thus, at $T_1 > T^* \approx T_c$, all the TLS's due to fast thermal activation processes release during the cooling from T_1 to T_c and do not contribute to the heat release; i.e., the heat release is independent of T_1 at $T_1 > T^* \approx T_c$. The TLS's are freezing at $T \leq T^*$, and then (at $T_0 < T_c$) they give the usual contribution to the heat release as a result of tunneling through the barrier. The main contribution to the heat release for $T_0 < T_c < T_1$ comes from TLS's with the freezing temperatures $T^* \approx T_c$.

The idea that a thermal depopulation of the TLS's is responsible for the saturation of the heat release with increasing of the charging temperature T_1 has been pronounced in Ref. 6 and approved in Ref. 19. However, authors of Ref. 6 supposed that this phenomenon results from the thermal depopulation of high-energy states and proposed to describe it using an energy-dependent density of states. In our consideration the density of states (3.6) as a function of the energy and barrier height is constant in the tunneling region. The relaxation rate (2.13) in the thermal activation region does not depend on the energy, either. And our explanation is that *the TLS's with nearly the same freezing temperatures (and barrier heights) are responsible for the heat release at low temperatures* $T_0 < T_c$. During cooling from T_1 to T_c, all these TLS's are in the thermal equilibrium with the lattice due to fast thermal activation processes (thermal depopulation, but with the rate independing of the energy). As to TLS's with higher barriers (and higher freezing temperatures), they do not contribute to the heat release at all (at least on the experimental time scale).

The calculated parameters V, T^*, and T_c of a-SiO_2 and $LiCl \cdot 7H_2O$ for relaxation times and a cooling rate typical for heat-release experiments are given in Table I. The characteristic energy W was calculated from (2.16) and experimental values of $T_{\min}$. For calculation of $\tau(E)$ (2.12) (at $E = kT^*$) the value of $K_3 = 4k^3\gamma^2/\pi\rho\hbar^4 v^5$ determined from ultrasonic experiments[34,35] was used [see (3.8) and (2.12)]:

$$\tau_{\min}(E) = \frac{8k^3}{K_3 E^3}\tanh\frac{E}{2kT} ,$$
$$\tau(E) = \tau_{\min}(E)\left[\frac{E}{W}\right]^2 . \tag{3.35}$$

Both the crossover temperature T_c and freezing temperature T^* are nearly constant in the time scale typical of heat-release experiments. Thus our consideration predicts a sharp transition of the T_1 dependence of the heat release at

$$T_1 \approx T^* \approx (1.1\text{–}1.4)T_c . \tag{3.36}$$

Since the crossover and freezing temperatures in this case are proportional to the characteristic energy W, the abso-

TABLE I. Calculated values V (potential barrier height), T^* (freezing temperature), and T_c (crossover temperature) for a-SiO_2 and $LiCl \cdot 7H_2O$ for relaxation times τ and cooling rate ($|R^*| = 10^{-2}$ K/s) typical for heat-release experiments [Eqs. (2.15), (3.31), (3.32), and (3.34)]. The characteristic energy W was deduced from the temperature $T_{\min}$, where a minimum of the function $C(T)/T^3$ was observed [Eq. (2.16)]. $C(T)$ is the measured specific heat. The coefficient K_3 was determined from ultrasonic experiments (Refs. 34 and 35). $\tau_0 = 10^{-12}$ s.

Material	a-SiO_2		$LiCl \cdot 7H_2O$	
W/k (K)	4		14	
K_3 (10^9 s/K^3)	0.4		4.44	
τ (s)	10^3	10^6	10^3	10^6
V/k (K)	100	130	445	570
T^* (K)	3.3	4.3	14	18
T_c (K)	2.8	3.2	13	13.7
kT^*/W	0.82	1.1	1.0	1.3
kT_c/W	0.71	0.8	0.9	0.98
T^*/T_c	1.15	1.37	1.1	1.3

lute values of these parameters differ for various materials. However, the ratios T^*/T_c, kT^*/W, and kT_c/W remain nearly unchanged even for larger value of the energy W (see Table I).

In our consideration we have not taken into account the existence of a maximum barrier height $V_{\max}$ in the distribution function (3.6) [or (3.16)]. As we can see from Table I, the barrier heights of the TLS's responsible for the heat release in a-SiO_2 are much smaller than $V_{\max}/k \simeq 500$ K obtained from the position of the relaxation absorption peak.[20] Therefore the idea that the cutoff in the barrier distribution [or $(\Delta_0/E)_{\min}=5\times10^{-8}$ (Refs. 19 and 36)] is responsible for the saturation of the heat release with increasing of the charging temperature T_1 in the particular case of a-SiO_2 contradicts with the experiments on relaxation ultrasound absorption.[20] The barrier height $V=V_{\max}=k(500\ \text{K})$ corresponds to $(\Delta_0/W)_{\min}\simeq 2\times10^{-22}$ [see (2.4) and (2.8) for $W/k=4$ K] and to tunneling relaxation times $\tau\simeq 6\times10^{24}$ yr [see (2.11)] with $\tau(E)\simeq 10^{-11}$ s.

IV. COMPARISON WITH EXPERIMENT

A. Tunneling range ($T_0, T_1 < T_c$)

The most heat-release data in the tunneling range are in a good agreement with the standard tunneling theory of AHVP, except for some organic materials, where other time dependences were observed.[8-10] Therefore a direct comparison between the SPM and the AHVP model is reasonable.

The AHVP model yields, for the specific heat and the heat release,

$$C(T)=\frac{\pi^2k^2}{12}\mathcal{V}\bar{P}T\ln\frac{4t}{\tau_{\min}(kT)}\ , \tag{4.1}$$

$$\dot{Q}=\frac{\pi^2k^2}{24}\mathcal{V}\bar{P}\frac{T_1^2-T_0^2}{t}\ , \tag{4.2}$$

where $\bar{P}$ is a constant density of states of the TLS's. Thus the density of states $\bar{P}$ can be obtained both from the specific heat (P_C) and the heat release (P_Q):

$$P_C=\frac{12}{\pi^2k^2}\frac{C(T)}{\mathcal{V}T\ln[4t/\tau_{\min}(kT)]}\ , \tag{4.3}$$

$$P_Q=\frac{24}{\pi^2k^2}\frac{\dot{Q}t}{\mathcal{V}(T_1^2-T_0^2)}\ . \tag{4.4}$$

In the SPM the specific heat is determined by[25]

$$C(T)=\pi^2k^2\left[\frac{2}{9}\right]^{1/3}\frac{\mathcal{P}_0\eta_L^{5/2}}{W}T\mathcal{V}\times\ln^{1/3}\left[\frac{W}{kT}\left[\frac{t}{\tau_{\min}(kT)}\right]^{1/2}\right]\ , \tag{4.5}$$

and the heat release is determined by (3.11). As a result, we obtain

$$P_C=F_1(T,t)\frac{\mathcal{P}_0\eta_L^{5/2}}{W}\ , \tag{4.6}$$

$$P_Q=F_2(T_1,T_0,t)\frac{\mathcal{P}_0\eta_L^{5/2}}{W}\ , \tag{4.7}$$

where

$$F_1(T,t)=12\left[\frac{2}{9}\right]^{1/3}\left\{\ln^{1/3}\left[\frac{W}{kT}\left[\frac{t}{\tau_{\min}(kT)}\right]^{1/2}\right]\Big/\ln\frac{4t}{\tau_{\min}(kT)}\right\}\ , \tag{4.8}$$

and

$$F_2(T_1,T_0,t)=2\left[\frac{2}{9}\right]^{1/3}\frac{T_1^2f(T_1,t)-T_0^2f(T_0,t)}{T_1^2-T_0^2}\ . \tag{4.9}$$

Both theories agree with each other if $F_1(T,t)=F_2(T_1,T_0,t)=\text{const}$, since $P_C=P_Q=\bar{P}$ in the AHVP model. The calculated values of $F_1(T,t)$ and $F_2(T_1,T_0,t)$ are given in Tables II–IV for a-SiO_2 and $LiCl\cdot7H_2O$ and for typical parameters T, T_1, T_0, and t of specific-heat and heat-release measurements. It is seen that the functions $F_1(T,t)$ and $F_2(T_1,T_0,t)$ show weak time and temperature dependences only. Thus the SPM leads nearly to the same time and temperature depen-

TABLE II. Calculated values of $F_1(T,t)$ for a-SiO_2 [Eq. (4.8)] with $W/k=4$ K, $K_3=0.4\times10^9\ \text{s K}^{-3}$ (Ref. 34) and for $LiCl\cdot7H_2O$ [$W/k=14$ K, $K_3=4.44\times10^9\ \text{s K}^{-3}$ (Ref. 35)] for parameters t and T typical for the specific heat measurements.

Material	a-SiO_2				$LiCl\cdot7H_2O$	
T (K)	0.1	1.0	0.1	1.0	1.0	8.0
t (s)	10^2	10^2	10^4	10^4	10^2	10^2
$F_1(T,t)$	0.94	0.70	0.79	0.62	0.67	0.56
$\bar{F}_1(T,10^2\ \text{s})$	0.82 ± 0.12				0.62 ± 0.05	

TABLE III. Calculated values of $F_2(T_1,T_0,t)$ for a-SiO_2 [Eq. (4.9)] with $W/k=4$ K, $K_3=0.4\times10^9$ s K^{-3} for parameters T_1, T_0, and t typical for heat-release measurements.

T_1 (K)	1.8	1.8	1.8	1.8	3.6	3.6	3.6	3.6
T_0 (K)	0.1	0.1	1.0	1.0	0.1	0.1	1.0	1.0
t (s)	10^4	10^6	10^4	10^6	10^4	10^6	10^4	10^6
$F_2(T_1,T_0,t)$	0.195	0.177	0.193	0.177	0.192	0.175	0.191	0.175
$\bar{F}_2(1.8\text{ K},T_0,t)$				0.186±0.009				

dences of the heat release as the AHVP model. The registration of these differences between the models requires precision specific-heat and heat-release measurements. However, the absolute value of F_1 is about 4 times larger than the absolute value of F_2 (see Tables II–IV). If the SPM is correct, we expect $P_C\approx4P_Q$ in contradiction to the AHVP model, where $P_C=P_Q=\bar{P}$.

Up to now, comparable heat-release and specific-heat data exist for a-SiO_2 and $LiCl\cdot7H_2O$ only. For both materials the density of states, P_C, calculated from the specific-heat data is clearly larger than the density of states, P_Q, obtained from the heat-release experiments (see Table V); i.e., the experimental results are in better agreement with the SPM. More experimental data are necessary to prove this interesting fact.

B. Intermediate range ($T_0<T_c<T_1$)

Our consideration predicts a sharp transition of the heat-release temperature dependences at $T_1\approx T^*\approx(1.1-1.4)T_c$: $\dot{Q}\propto T_1^2-T_0^2$ at $T_1<T^*$ and $\dot{Q}\propto T_*^2-T_0^2$ at $T_1>T^*$ (i.e., $\dot{Q}$ does not depend on T_1 in this case).

Figure 1 shows the heat-release data of various amorphous and glasslike crystalline materials in the representation $\dot{Q}/\dot{Q}_t$ as a function of T_1/T_{1c}. $\dot{Q}_t$ is the calculated value in the tunneling range [see (3.11)]. The parameters $\mathcal{P}_0\eta_L^{5/2}/W$ and T_{1c} are given in Table VI. For the organic materials, where $\dot{Q}$ is not proportional to t^{-1}, $\dot{Q}/\dot{Q}_t$ was determined for $t=1$ h, neglecting the deviation from the t^{-1} law. T_{1c} is the upper limit of T_1, where the temperature dependence corresponds to the tunneling range; i.e., $\dot{Q}$ is proportional to $T_1^2-T_0^2$. We see that the expected sharp transition is not observed: $\dot{Q}$ is independent of T_1 at $T_1>8T_{1c}$ only (where $\dot{Q}/\dot{Q}_t$ is proportional to T_1^{-2}); i.e., the transition extends from T_{1c} to about $8T_{1c}$.

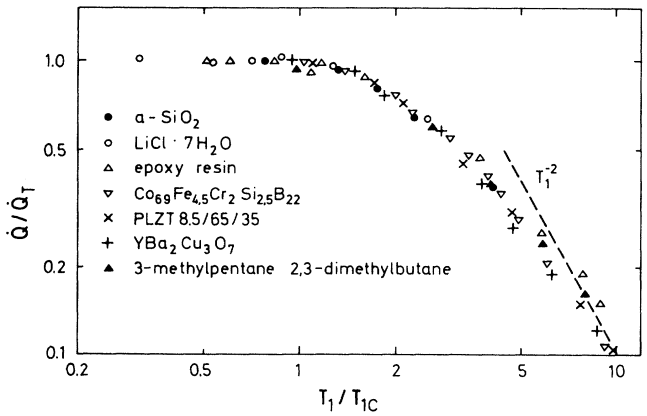

FIG. 1. Heat release of various amorphous and glasslike crystalline materials for references (see Table VI) in the representation $\dot{Q}(T_1,T_0,t)/\dot{Q}_t$ as a function of T_1/T_{1c} at $T_0<T_c$. $\dot{Q}_t$ is the calculated heat release in the tunneling range [Eq. (3.11)]. T_{1c} is the upper limit of T_1, where $\dot{Q}$ is proportional to $T_1^2-T_0^2$ (see Table VI).

On the other hand, for all the materials and $T_0<T_{1c}$ the time dependence does not change from $T_1<T_{1c}$ to $T_1>T_{1c}$ case. This means that the thermal activation processes at $T_0<T_{1c}$ are frozen in and the tunneling processes are responsible for the heat release. Therefore the absence of the sharp transition at T^* can be understood if there is a distribution of the values of W (and correspondingly of T^* and T_c) in the glass.

The distribution function $G(T^*)$ [or $G(W)$] can be evaluated from the experimental curve $\dot{Q}(T_1^2)$. The distribution function $G(T^{*2})$ coincides with the absolute value of the second derivative of the function $\dot{Q}(T_1^2)$ on its argument T_1^2 (see the Appendix) and $G(T^*)=2T^*G(T^{*2})$. Since with

$$\dot{Q}(T_1^2)=A\tanh aT_1^2+B\tanh bT_1^2+C\tanh cT_1^2 \tag{4.10}$$

we have found a good fit of the experimental curves $\dot{Q}(T_1^2)$ for nine different materials (see Figs. 2 and 3, where we present two of them), it is possible to give an analytical expression of $G(T^*)$:

$$G(T^*)=\frac{4T^*}{Q_0}\left[Aa^2\frac{\tanh aT^{*2}}{\cosh^2aT^{*2}}+Bb^2\frac{\tanh bT^{*2}}{\cosh^2bT^{*2}}+Cc^2\frac{\tanh cT^{*2}}{\cosh^2cT^{*2}}\right], \tag{4.11}$$

where Q_0 is determined by (A3), $Q_0=Aa+Bb+Cc$, and

TABLE IV. Calculated values of $F_2(T_1,T_0,t)$ for $LiCl\cdot7H_2O$ [Eq. (4.9)] with $W/k=14$ K, $K_3=4.44\times10^9$ s K^{-3} for parameters T_1, T_0, and t typical for heat-release measurements.

T_1 (K)	2.5	2.5	7.0	7.0
T_0 (K)	1.5	1.5	1.5	1.5
t (s)	2×10^3	4×10^4	2×10^3	4×10^4
$F_2(T_1,T_0,t)$	0.18	0.17	0.177	0.168
$\bar{F}_2(T_1,1.5\text{ K},t)$		0.174±0.006		

TABLE V. Comparison between the calculated specific heat and heat release with the experimental data for a-SiO_2 and $LiCl{\cdot}7H_2O$. P_C and P_Q are the density of states in the AHVP model deduced from the specific-heat (P_C) and heat-release (P_Q) measurements. For the functions $F_1(T,t)$ and $F_2(T_1,T_0,t)$, see Eqs. (4.8) and (4.9) and Tables II–IV. The SPM predicts $F_1(T,t)/F_2(T_1,T_0,t)=P_C/P_Q>1$ in contradiction to the AHVP model.

Material	a-SiO_2	$LiCl{\cdot}7H_2O$
P_C (10^{44}/J m^3)	5.3[a]	31±6[b]
	7.5[a]	
P_Q (10^{44}/J m^3)	1.0[c]	10.1±0.3[b]
	3.0[d]	
P_C/P_Q	1.8–7.5	3.1±0.7
$\bar{F}_1(T,10^2$ s)	0.82±0.12	0.62±0.05
$\bar{F}_2(T_1,T_0,t)$	0.186±0.009	0.174±0.006
$\bar{F}_1/\bar{F}_2$	4.4±0.8	3.5±0.4

[a]References 37 and 38.
[b]Reference 11.
[c]Reference 6.
[d]Reference 4.

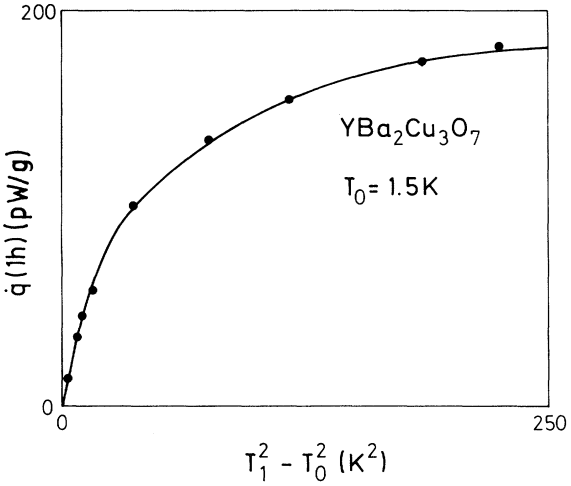

FIG. 2. Heat release from an $YBa_2Cu_3O_7$ sample 1 h after the start of cool down as a function of the charging temperature T_1. The solid circles are data from Ref. 15. The line is the fit using (4.10) with $A=66.7$ pW/g, $a=5.4\times10^{-2}$ K^{-2}, $B=118$ pW/g, $b=8.33\times10^{-3}$ K^{-2}, and $C=0$.

the coefficients A, a, B, b, C, c, etc., are chosen to obtain a good fit.

The physical reason for such a form of the fitting function (4.10) is that the corresponding distribution function (4.11) is a linear combination of functions, each of them differing very slightly ($\leq 5\%$) from the Gaussian distribution with the same dispersion and position of the maximum,

$$f(x)\equiv 4x\frac{\tanh x^2}{\cosh^2 x^2}\approx\frac{1}{\sqrt{2\pi}\delta}\exp\left[-\frac{(x-x_m)^2}{2\delta^2}\right], \quad (4.12)$$

where $x_m=0.915$ and $\delta=0.304$ are position of the maximum and dispersion of the function $f(x)$, respectively.

In Figs. 4–7 are shown the obtained distribution functions $G(T^*)$ of $YBa_2Cu_3O_7$, a-SiO_2, and $LiCl{\cdot}7H_2O$ and of the metallic glass $Co_{69}Fe_{4.5}Cr_2Si_{2.5}B_{22}$. Similar distribution functions were obtained for other amorphous and glasslike crystalline solids too (for their parameters, see Table VI). In the common case, the distribution function has several peaks. The first one usually has the biggest

TABLE VI. Parameters of the distribution function of the freezing temperature in different materials obtained from the heat-release data. T^*_{m1}, T^*_{m2}, and T^*_{m3} are the positions of the peaks in the distribution function (in parentheses the concentration of TLS's of corresponding type is given). $T^*_{\rm av}$ is the average value of the freezing temperature. W/k is the value of the characteristic energy in the SPM deduced from position of the first peak in $G(T^*)$ and data of Table I ($t=10^3$ s). $\mathcal{P}_0\eta_L^{5/2}/W$ is the value characterizing the density of states in the SPM [see (3.6)]. $T_{\rm min}$ is the temperature where the minimum of the function $C(T)/T^3$ was observed, $C(T)$ is the measured specific heat, and T_{1c} is the upper limit of the charging temperature T_1, where the experimental heat-releast data agree with Eq. (3.11). Except $T_{\rm min}$, all parameters were deduced from the heat-release data [see Eqs. (4.10), (4.11), and (4.13) and Table I].

Material	$T_{\rm min}$ (K)	T_{1c} (K)	T^*_{m1} (K)	T^*_{m2} (K)	T^*_{m3} (K)	$T^*_{\rm av}$ (K)	W/k (K)	$\mathcal{P}_0\eta_L^{5/2}/W$ (10^{44}/J m^3)
a-SiO_2[a]	2.0	2.0	3.5 (78%)	20.9 (13%)	24.2 (9%)	7.9	4.3	5.6
$LiCl{\cdot}7H_2O$[b]	7.0	8.0	16.1 (100%)			16.8	16.1	63
$Fe_{80}B_{14}Si_6$[c]		3.3	4.76 (68%)	11.9 (32%)		7.36		8.3
$Co_{69}Fe_{4.5}Cr_2Si_{2.5}B_{22}$[d]		4.0	4.1 (33%)	9.61 (56%)	20.5 (11%)	9.35		5.0
Epoxy resin[e]	1.4	2.5	4.56 (79%)	15.9 (21%)		7.3		43
Pentanol-2[f]		3.8	5.61 (55%)	13.6 (45%)		9.5		23
3-methylpentane–(2,3)-dimethylbutane[g]		2.5	4.1 (79%)	13.9 (21%)		6.39		100
$YBa_2Cu_3O_7$[h]		2.3	3.9 (79%)	10 (21%)		5.46		24
$Pb_{0.915}La_{0.085}(Zr_{0.65}Ti_{0.35})O_3$[i]	2.0	1.3	2.05 (67%)	4.1 (24%)	10.0 (9%)	3.4		67

[a]Reference 6.
[b]Reference 11.
[c]References 12 and 13.
[d]Reference 13.
[e]Reference 9.
[f]Reference 10.
[g]Reference 8.
[h]References 14–16.
[i]References 17 and 18.

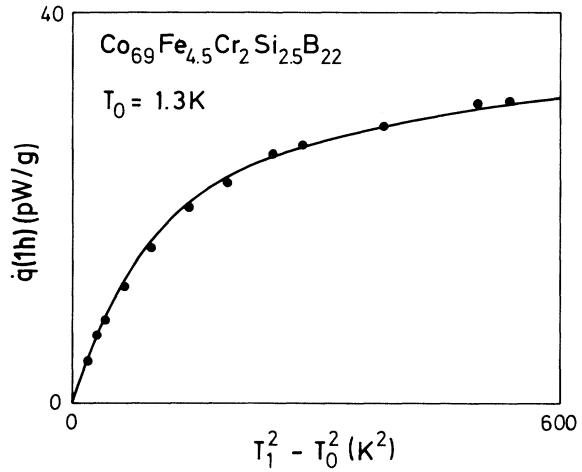

FIG. 3. Heat release from a $Co_{69}Fe_{4.5}Cr_2Si_{2.5}B_{22}$ sample 1 h after the start of cool down as a function of the charging temperature T_1. The solid circles are data from Ref. 13. The line is the fit using (4.10) with $A=1.8$ pW/g, $a=5\times10^{-2}$ K^{-2}, $B=17$ pW/g, $b=9.09\times10^{-3}$ K^{-2}, $C=15$ pW/g, and $c=2.0\times10^{-3}$ K^{-2}.

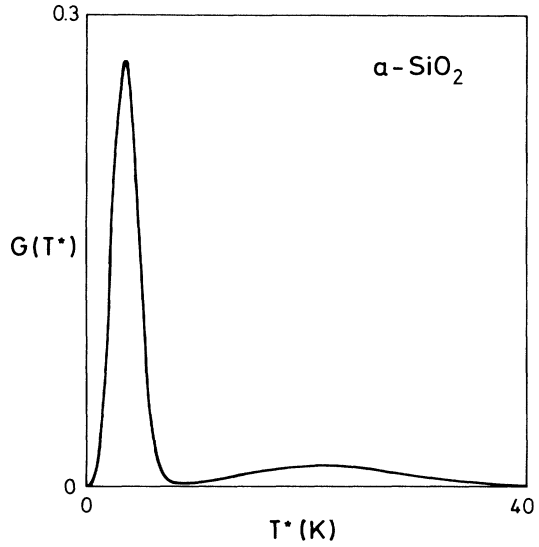

FIG. 5. Distribution function of the freezing temperature $G(T^*)$ in a-SiO_2. Experimental data are taken from Ref. 6. Fitting parameters in (4.10): $A=11.5$ pW/g, $a=6.8\times10^{-2}$ K^{-2}, $B=70$ pW/g, $b=1.92\times10^{-3}$ K^{-2}, $C=60$ pW/g, and $c=1.43\times10^{-3}$ K^{-2}.

amplitude and its position correlates with the value of W obtained from specific-heat measurements (see Table VI). One can believe that these peaks correspond to the contribution from different types of two-level systems. From parameters A,a,B,b,C,c, we can calculate their concentration n_1, n_2, and n_3:

$$n_1=\frac{Aa}{Q_0},\quad n_2=\frac{Bb}{Q_0},\quad n_3=\frac{Cc}{Q_0}\ . \tag{4.13}$$

In Table VI we also give the average values of the freezing temperature T^*_{av}, which is not sensitive to the form of the approximating function [see (A6)]. For all the investigated materials, we obtained $T^*_{av}/T_{1c}\approx3\pm1$, which explains the universal behavior of the heat release of these materials in Fig. 1.

It is noteworthy that the specific-heat and ultrasonic-absorption data in the thermal activation region will be

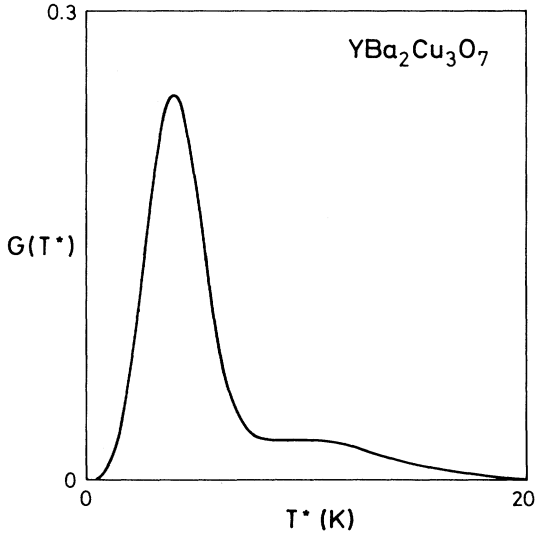

FIG. 4. Distribution function of the freezing temperature $G(T^*)$ in $YBa_2Cu_3O_7$. Fitting parameters are given in the caption to Fig. 2.

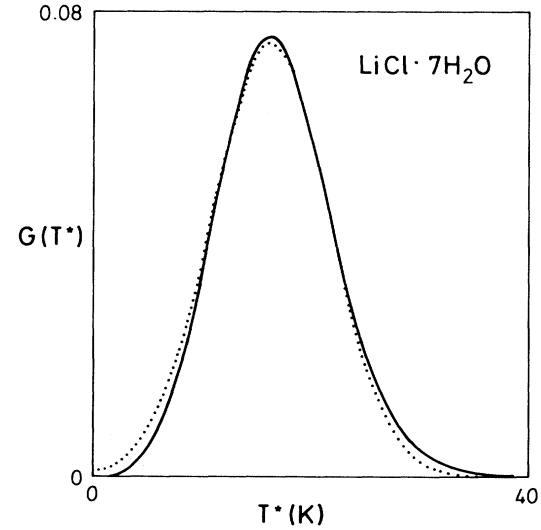

FIG. 6. Distribution function of the freezing temperature $G(T^*)$ in $LiCl\cdot7H_2O$. Experimental data are taken from Ref. 11. Fitting parameters in (4.10): $A=732$ nW, $a=3.23\times10^{-3}$ K^{-2}, and $B=C=0$. Dots show the Gaussian distribution with the same position of the maximum and dispersion $\delta T^*=5.35$ K [see (4.12)].

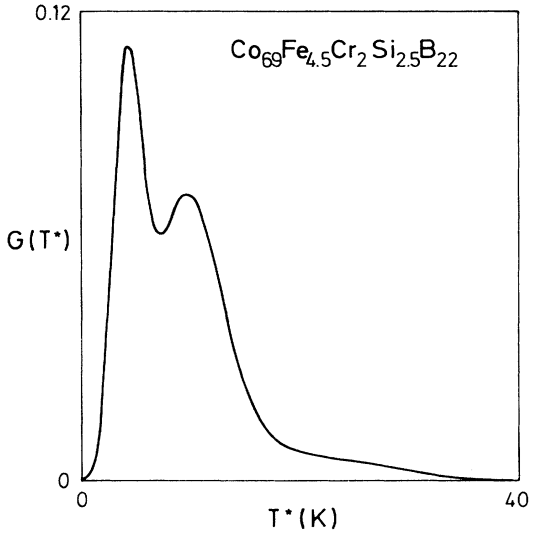

FIG. 7. Distribution function of the freezing temperature $G(T^*)$ in $Co_{69}Fe_{4.5}Cr_2Si_{2.5}B_{22}$. Fitting parameters are given in the caption to Fig. 3.

influenced by the main peak of the corresponding distribution function $G(W)$. However, it is difficult to obtain the distribution function from these experiments, whereas the heat release is very sensitive to existence of TLS's with large value of T^* (or W). Even a small number of such TLS's yields a marked contribution to $\dot{Q}$ because of their large energies.

The physical reason for the distribution of W within one peak can be either the distribution of binding energy $\mathcal{E}_0$ or the distribution of the effective mass of the tunneling entity M because probably a large number of particles are responsible for a "dressing" of the moving atom.[39,40] The different peaks could be caused by a different geometry of the tunneling entities.[39]

C. Thermal activation range ($T_c < T_0, T_1$)

The heat release in the thermal activation range is *de facto* unexplored. Since

$$T_c \approx (0.7-0.9)T^* , \tag{4.14}$$

heat-release measurements at $T_0 > 3$ K are required for the most investigated materials (see Table VI). Such experiments are quite difficult, because the sensitivity of the heat-release measurements decreases rapidly with increasing of T_0. Up to now, only two experiments were performed in this temperature range with the glasslike crystalline material $YBa_2Cu_3O_7$ (Refs. 14–16) and the epoxy resin.[9]

At $T_0 = 1.5$ K the heat release of $YBa_2Cu_3O_7$ is proportional to t^{-1} and the T_1 dependence yields $T_{1c} = 2.3$ K ($T_c \approx 3.5$ K, $W/k \approx 5.0$ K; see Fig. 1 and Tables I and VI). The heat release was measured after cooling a sample from $T_1 = 201$ K to various T_0 ($1.56 \le T_0 \le 4.25$ K) also. At $T_0 = 3.2$ K about 30% of TLS's have $T_c < T_0$ (see Fig. 4) and the heat release is proportional to $t^{-0.7}$ (see Fig. 8) in a good agreement with (3.28), which predicts $\dot{Q}$ to be proportional to $t^{-0.76}$. Moreover, the absolute value of $\dot{Q}$ increases with increasing T_0 in agreement qualitatively with (3.28), while the heat release decreases with T_0 in the tunneling and the intermediate ranges.

It is not surprising that the influence of the thermal activation starts at a much lower temperature than $T_c \approx 3.5$ K. Since T_c and T^* have the same distribution (proportional to the distribution function of W), we expect to register the first influence of the thermal activation at $T_0 \approx 2.3$ K (when about 10% of TLS's have $T_c < T_0$). It may be thought that an up-down motion of $\dot{Q}$ for $t > 2\times10^5$ s and $T_0 = 4.25$ K can be explained by the thermal activation processes if there is a cutoff in the barrier-height distribution at $V \approx 170$ K [see (3.19) for $T_0 = 4.25$ K and $\tau_0 = 10^{-12}$ s]. But, at first, the cutoff should be unbelievably steep. And, second, the ultrasound-absorption data[41] indicate that there is no cutoff in this barrier-height region. The position of ultrasound-absorption relaxation peak about 36 K (for frequency 1.06 kHz) corresponds to a cutoff in the barrier-height distribution at $V/k \approx 700-800$ K only. The only difference between heat-release experiments[16] and the ultrasound one[41] is the different time scale. In the former case, the time scale is about 2×10^5 s and in the last one it is only 10^{-3} s. The steepest of the up-down motion indicates some fast reconstruction of the whole sample (like the first-order phase transition). But more experimental data are necessary to prove this fact.

From Fig. 8 ($T_0 = 1.56$ K), we also see another interesting fact: The heat release is proportional to t^{-1} for $t < 2\times10^4$ s and proportional to $t^{-0.7}$ for $t > 5\times10^4$ s.

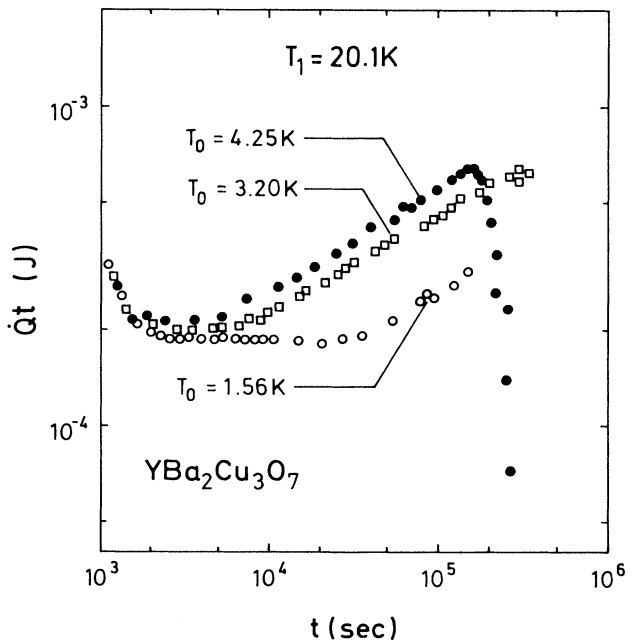

FIG. 8. Heat release $\dot{Q}(T_1, T_0, t)$ after cooling of $YBa_2Cu_3O_7$ from the equilibrium temperature $T_1 = 20.1$ K to various T_0 ($1.56 \le T_0 \le 4.25$ K) as a function of time t (Ref. 16).

Because of $\dot{Q} \propto T^{*2} - T_0^2$, the freezing temperature in the short-time range appears to be smaller than in the long-time range. It correlates with data from Table I [and (3.31)], where one can see that the freezing temperature (and the barrier height of the relevant TLS's) increases with time slowly. However, the behavior of crystalline $YBa_2Cu_3O_7$ may be not typical for amorphous systems. Therefore analogous experiments must be performed with amorphous solids (for example, with a-SiO_2, where $T_{1c} \approx 2.0$ K, $T_c \approx 3.2$ K).

For some noncrystalline organic materials (epoxy resin, pentanol-2, 2-methylpentane/2,3-dimethylbutane), $\dot{Q}$ is proportional to t^{-a} with $a = 0.66-0.76$ even at temperatures below 2 K.[8-10] However, some facts indicate that this time dependence is not caused by the thermal activation: (1) The T_1 dependence for these materials yields T_{1c} values not far from the corresponding value for a-SiO_2 (see Table VI), i.e., $T_c \approx 3.7-5$ K. (2) The time dependence ($\dot{Q} \propto t^{-0.7}$) was found for epoxy resin at $T_0 = 1.0$ K,[9] as well as at $T_0 = 0.05$ K.[6]

Nevertheless, the thermal activation processes seem to be responsible for the following phenomenon. For the epoxy resin, not only the heat release after cooling but also the heat absorption after rapid heating was measured. In the tunneling range ($T_0, T_1 < 1.4$ K) in both experiments, the same absolute values and the same time dependences were observed (see Fig. 9) in agreement with tunneling theory. However, if one temperature is lower and another one higher than ≈ 1.4 K, there are differences between heat release and heat absorption. After cooling, the temperature $T_0 < 1.4$ K and we are in the tunneling range. After heating $T_0 > 1.4$ K and, for some part of TLS's, thermal activation processes dominate. And though we did not consider here a theory of the heat absorption in the thermal activation region (this theme deserves a separate consideration), we mention some interesting experimental facts. The time dependence changes from $\dot{Q} \propto t^{-0.76}$ in the tunneling range ($T_0 < 1.4$ K) to $\dot{Q} \propto t^{-0.62}$ at $T_0 = 1.92$ K; the absolute value of the heat absorption is larger than the value of the heat release. At $T_0 > 1.92$ K the time dependence changes again and the relaxation is faster than $t^{-0.62}$. For the epoxy resin, the heat absorption was measured for a nearly constant $\Delta T = T_1 - T_0 \approx 0.5$ K also. The heat absorption at $T_0 > 1.6$ K is roughly proportional to $T_0^2(T_1 - T_0)$ (see Ref. 9 and Figs. 9 and 10).

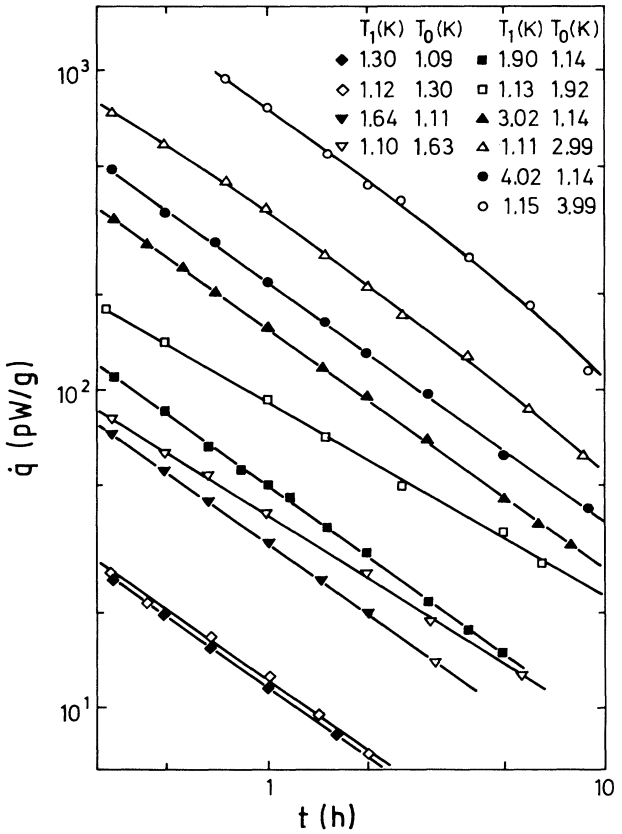

FIG. 9. Heat release (solid dots) after cooling and the absolute value of the heat absorption after heating (open dots) of a epoxy resin sample from T_1 to T_0 as a function of time t.

Our analysis shows that the available experimental heat-release data in the thermal activation range agree qualitatively and partially quantitatively with our consideration if we take into account a distribution of the characteristic energy W and correspondingly of the freezing temperature T_f and crossover temperature T_c. For a closer examination of our theory, more experimental data are necessary.

V. CONCLUSION

Using the soft-potential model, we developed a general theory of heat release in glasses which explains numerous experiments in a wide temperature region. In the low-temperature region, the temperature and time dependences nearly coincide with the predictions of the standard tunneling model of AHVP. However, the SPM predicts that the density of states obtained from specific heat is about a factor of 4 bigger than the density of states calculated from the heat-release data (if one uses the AHVP model). In the higher-temperature range (more than a few kelvin), the thermal activation processes in frozen-in TLS's are responsible for the heat release and determine its time and temperature dependences. The crossover temperature T_c between tunneling and activation appears to be of the order of a few kelvin only. Its value is determined by the characteristic energy W in the soft atomic potentials, which is related to position of the minimum in the temperature dependence of the specific heat $C(T)/T^3$. It is shown that a distribution of this energy should exist to explain the experimental data. The distribution function obtained from the heat-release data has several peaks which correspond probably to different types of two-level systems in the material.

ACKNOWLEDGMENTS

Useful discussions with U Buchenau, P. Esquinazi, E. Hegenbarth, S. Hunklinger, V. G. Karpov, G. Kasper, H. v. Löhneysen, G. Mattausch, M. Meissner, F. Pobell, and

G. Weiss are gratefully acknowledged. One of us (D.A.P.) thanks the Alexander von Humboldt Foundation for financial support and Institute für Angewandte Physik, Heidelberg for hospitality during his stay in Germany.

APPENDIX

Let us, for simplicity, consider the case when $T_0=0$. Then the dependence of the heat release $\dot{Q}$ from the charging temperature $x=T_1^2$ is given by

$$\dot{Q}(x)=Q_0\int_0^\infty dy\, G(y)[x\Theta(y-x)+y\Theta(x-y)] , \quad \text{(A1)}$$

where the distribution function of the freezing temperature squared $G(y)(y=T^{*2})$ is normalized to unity,

$$\int_0^\infty dy\, G(y)=1 \quad \text{(A2)}$$

and

$$Q_0=\left.\frac{d\dot{Q}(x)}{dx}\right|_{x=0} . \quad \text{(A3)}$$

From (A1) and (A2), we have

$$\frac{\dot{Q}(x)}{Q_0}=x-\int_0^x dy\,(x-y)G(y) . \quad \text{(A4)}$$

And from (A4) we obtain

$$G(x)=-\frac{1}{Q_0}\frac{d^2\dot{Q}}{dx^2} . \quad \text{(A5)}$$

From the experimental curve $\dot{Q}(T_1^2)$, one can determine also the average value of the freezing temperature $T_{\rm av}^*$,

$$T_{\rm av}^*=\frac{1}{2Q_0}\int_0^\infty dT_1\frac{\dot{Q}(T_1^2)}{T_1^2} . \quad \text{(A6)}$$

*On leave from St. Petersburg State Technical University, St. Petersburg, Politechnicheskaya 29, 195251, Russia.

[1]W. A. Phillips, Rep. Prog. Phys. **50**, 1657 (1987).
[2]P. W. Anderson, B. I. Halperin, and C. M. Varma, Philos. Mag. **25**, 1 (1972).
[3]W. A. Phillips, J. Low Temp. Phys. **7**, 351 (1972).
[4]J. Zimmermann and G. Weber, Phys. Rev. Lett. **46**, 661 (1981).
[5]M. T. Loponen, R. C. Dynes, V. Narayanamurti, and J. P. Carno, Phys. Rev. B **25**, 1161 (1982).
[6]M. Schwark, F. Pobell, M. Kubota, and R. M. Mueller, J. Low Temp. Phys. **58**, 171 (1985).
[7]S. Sahling, A. Sahling, and M. Koláč, Solid State Commun. **65**, 1031 (1988).
[8]S. Sahling (unpublished).
[9]M. Koláč, B. S. Neganov, A. Sahling, and S. Sahling, J. Low Temp. Phys. **68**, 285 (1987).
[10]E. I. Bunyatova, A. Sahling, and S. Sahling, Solid State Commun. **75**, 125 (1990).
[11]S. Sahling, Solid State Commun. **72**, 497 (1989).
[12]M. Koláč, B. S. Neganov, A. Sahling, and S. Sahling, Solid State Commun. **57**, 425 (1986).
[13]S. Sahling, A. Sahling, B. S. Neganov, and M. Koláč, J. Low Temp. Phys. **65**, 289 (1986).
[14]A. Sahling and S. Sahling, Mod. Phys. Lett. B **2**, 1327 (1988).
[15]A. Sahling and S. Sahling, J. Low Temp. Phys. **77**, 399 (1989).
[16]S. Sahling and J. Sievert, Solid State Commun. **75**, 237 (1990).
[17]S. Sahling, A. Sahling, B. S. Neganov, and M. Koláč, Solid State Commun. **59**, 643 (1986).
[18]S. Sahling, A. Sahling, and M. Koláč, J. Low Temp. Phys. **73**, 450 (1988).
[19]M. Deye and P. Esquinazi, Z. Phys. B **76**, 283 (1989).
[20]D. Tielbürger, R. Merz, R. Ehrenfels, and S. Hunklinger, Phys. Rev. B **45**, 2750 (1992).
[21]V. G. Karpov, M. I. Klinger, and F. N. Ignatiev, Zh. Eksp. Teor. Fiz. **84**, 760 (1983) [Sov. Phys. JETP **57**, 439 (1983)].
[22]V. G. Karpov and D. A. Parshin, Pis'ma Zh. Eksp. Teor. Fiz. **38**, 536 (1983) [JETP Lett. **38**, 648 (1983)].
[23]M. A. Il'in, V. G. Karpow, and D. A. Parshin, Zh. Eksp. Teor. Fiz. **92**, 291 (1987) [Sov. Phys. JETP **65**, 165 (1987)].
[24]U. Buchenau, Yu. M. Galperin, V. L. Gurevich, and H. R. Shober, Phys. Rev. B **43**, 5039 (1991).
[25]D. A. Parshin (unpublished).
[26]U. Buchenau, Yu. M. Galperin, V. L. Gurevich, D. A. Parshin, M. A. Ramos, and H. R. Schober, Phys. Rev. B **46**, 2798 (1992).
[27]D. A. Parshin (unpublished).
[28]D. A. Parshin (unpublished).
[29]Yu. M. Galperin, V. L. Gurevich, and V. I. Kozub, Europhysics Lett. **10**, 753 (1989).
[30]M. Huang and J. P. Sethna, Phys. Rev. B **43**, 3245 (1991).
[31]S. A. Langer, J. P. Sethna, and E. R. Grannan, Phys. Rev. B **41**, 2261 (1990).
[32]J. J. Brey and A. Prados, Phys. Rev. B **43**, 8350 (1991).
[33]D. A. Parshin and A. Würger, Phys. Rev. B **46**, 762 (1992).
[34]J. F. Berret and M. Meissner, Z. Phys. B **70**, 65 (1988).
[35]V. Röhring, K. Runge, and G. Kasper, in *Phonons '89*, edited by S. Hunklinger, W. Ludwig, and G. Weiss (World Scientific, Singapore, 1990), Vol. 1, p. 477.
[36]M. Deye and P. Esquinazi, in *Phonons '89* (Ref. 35), Vol. 1, p. 468.
[37]J. C. Lasjaunias, A. Ravex, M. Vandorpe, and S. Hunklinger, Solid State Commun. **17**, 1045 (1975).
[38]R. C. Zeller and R. O. Pohl, Phys. Rev. B **4**, 2029 (1971).
[39]G. A. Dyadna, V. G. Karpov, and V. N. Solov'ev, Fiz. Tverd. Tela (Leningrad) **32**, 2661 (1990) [Sov. Phys. Solid State **32**, 1542 (1990)].
[40]H. R. Schober and B. B. Laird, Phys. Rev. B **44**, 6746 (1991).
[41]P. Esquinazi, C. Duran, C. Fainstein, and M. N. Regueiro, Phys. Rev. B **37**, 545 (1988).